Journal of Alloys and Compounds 512 (2012) 27–32

Contents lists available at SciVerse ScienceDirect

Journal of Alloys and Compounds

journal homepage: www.elsevier.com/locate/jallcom

Physical properties and characterization of Ag doped CdS thin films

N.A. Shah[a,*], A. Nazir[b], W. Mahmood[a], W.A.A. Syed[c], S. Butt[b], Z. Ali[d], A. Maqsood[b]

[a] Thin Films Technology Research Laboratory, Department of Physics, COMSATS Institute of Information Technology, Islamabad 45320, Pakistan
[b] School of Chemical and Materials Engineering, National University of Science and Technology, Islamabad 45320, Pakistan
[c] Department of Physics, International Islamic University, Islamabad 45320, Pakistan
[d] Optics Laboratory, Nilore, Islamabad 45320, Pakistan

ARTICLE INFO

Article history:
Received 10 October 2010
Received in revised form 20 August 2011
Accepted 25 August 2011
Available online 21 September 2011

Keywords:
Thin films
Coatings
Morphology
Cadmium sulfide

ABSTRACT

Thin films of cadmium sulfide with very well defined preferential orientation and relatively high absorption coefficient were fabricated by thermal evaporation technique. The research is focused to the fabrication and characterization of the compositional data of CdS thin films obtained by using X-ray diffraction, scanning electron microscope along with energy dispersive X-ray spectroscopy. The optical properties were studied by using a UV-VIS-NIR spectrophotometer. The effects of silver-doping by ion exchange process on the properties of as-deposited CdS thin films have been investigated.

© 2011 Elsevier B.V. All rights reserved.

1. Introduction

Cadmium sulfide (CdS) belonging to the II–VI compound semiconductor family has great potential in applications such as solar cells, optical detectors and optoelectronic devices [1–3]. The electrical and optical properties make it extremely useful as window layer material for many photovoltaic solar cell modules [4–7]. Furthermore CdS has remained a focus of the material science community due to its important band gap, conversion efficiency, high absorption coefficient, stability and last but not the least its significantly low cost [8]. The current transport mechanisms in CdS thin films have been reported [9] and there exists a vast literature covering theoretical and experimental studies of electronic band structure [10]. CdS has a wide and direct band gap (2.42 eV), n-type semiconducting material [11] and found in two crystalline forms; cubic (zinc-blend) phase and hexagonal (wurtzite) phase. The development of cubic or hexagonal phase depends on many features including the deposition techniques [12,13]. Efficiencies about 16% have been reported for CdTe/CdS thin films solar cells [14]. Generally CdS thin films have high electrical resistivity which is reduced by using different dopants. A number of deposition techniques are being used for the fabrication of CdS thin films including thermal evaporation, chemical bath deposition, vacuum evaporation, chemical vapour deposition, spray pyrolysis, metal organic vapour-phase epitaxy, closed space sublimation, photochemical deposition, radio frequency sputtering, vapour transport deposition, electro deposition, screen printing and pulsed laser deposition [15–23].

2. Experimental

CdS thin films were deposited on glass substrates. The size of glass substrates were 25 mm × 75 mm, which were cleaned for about 30 min in IPA bath by ultrasonic cleaner. The source material, CdS powder with 99.99% purity obtained from m/s Aldrich was kept in the graphite boat of the size 20 mm × 70 mm. A 1000 W halogen lamp provided heat to the source material, while the temperature was monitored with a controller with K-type thermocouple. The substrate was heated by another 500 W halogen lamp, attached with a thermocouple to measure the substrate temperature. The source and substrate temperatures were kept at 550 °C and 450 °C respectively. The pressure in the chamber was set to about 10^{-5} mbar with the help of a rotary pump and oil diffusion pump. Various deposition times were optimized for obtaining a variety of film thickness, given in Table 1. Thin films with thicknesses ranging from 248 to 860 nm were obtained. Finally the source and substrate lamps were switched off for cooling down to room temperature before opening the chamber.

The fabricated thin films were annealed at 450 °C for 30 min under vacuum. As a next step, these thin films were immersed in a low concentration (0.1 g/100 ml) $AgNO_3$–H_2O solution at room temperature for various periods of time. The immersed samples were annealed at 450 °C under vacuum for 30 min for maximum diffusion of silver into the thin films. The structures of the silver-doped samples were studied by XRD using Cu Kα (1.5418 Å) radiation with operating voltage/current of 40 kV. The microstructure of the samples was examined using scanning electron microscopy (SEM). The SEM accelerating voltage was 10 kV. The compositions of Cd, S and Ag of all the samples were measured with the help of energy dispersive X-ray spectroscopy (EDX) attached to the SEM, and given in Table 1. The optical properties including refractive index, film thickness and optical band gap were calculated from the transmission spectra between 300 and 2000 nm recorded by spectrophotometer.

* Corresponding author. Tel.: +92 519235038; fax: +92 514442805; mobile: +92 3215105363.
E-mail address: nabbasqureshi@yahoo.com (N.A. Shah).

0925-8388/$ – see front matter © 2011 Elsevier B.V. All rights reserved.
doi:10.1016/j.jallcom.2011.08.081

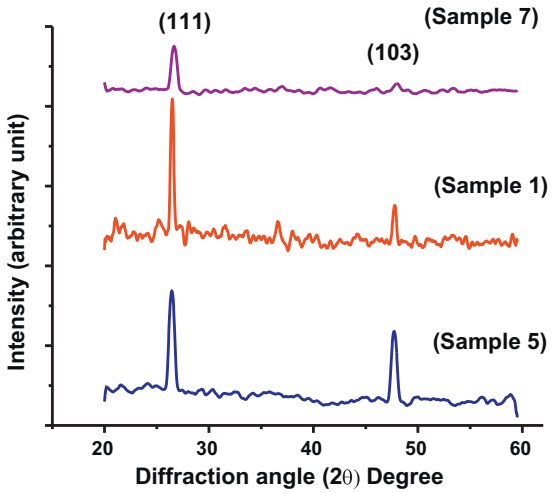

Fig. 1. The XRD spectra of as-deposited CdS thin film samples.

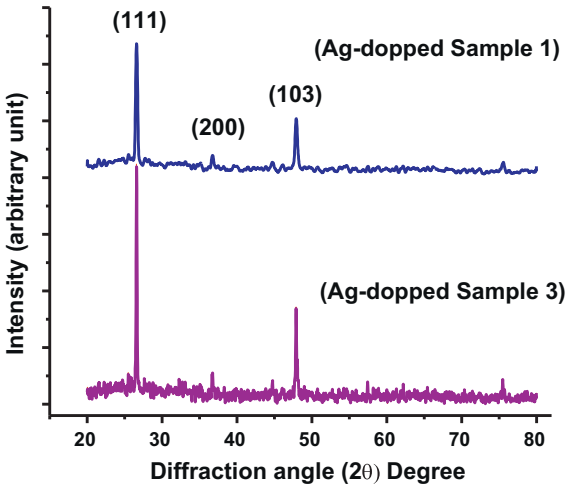

Fig. 2. The XRD patterns of Ag-doped CdS thin film samples.

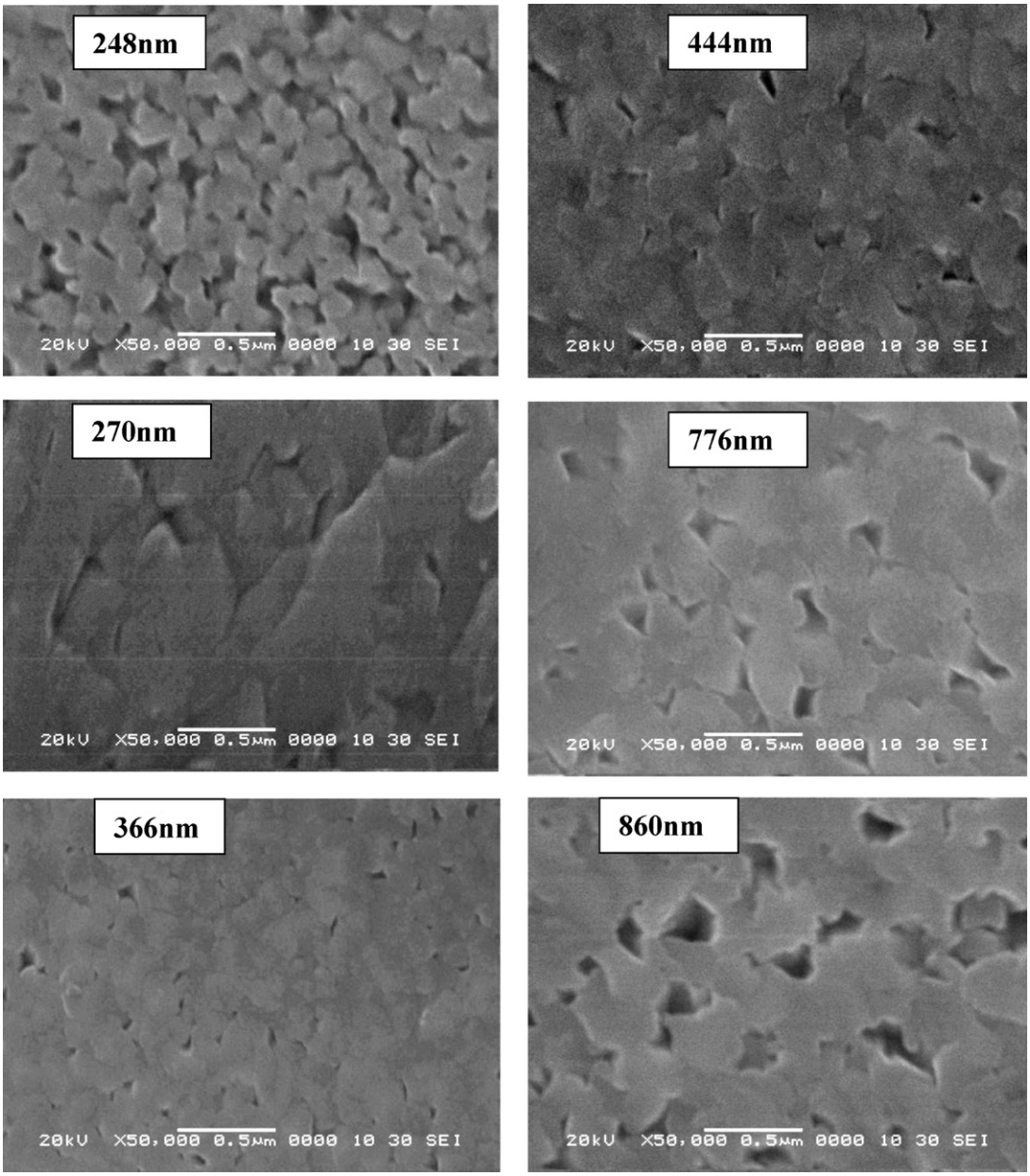

Fig. 3. SEM micrographs of as-deposited samples of different thicknesses.

In this research work, CdS thin films have been fabricated by thermal evaporation technique and furthermore, silver doping performed by ion exchange process; which is to our knowledge not reported earlier.

3. Results and discussion

3.1. Structural analysis

The structures of the as-deposited CdS and Ag-doped CdS thin films were studied using X-ray diffraction (XRD) technique. The diffraction spectra were measured at 2θ scanning mode ranging from 20 to 60 degree diffraction angle. The XRD spectra of as-deposited CdS thin films with different thicknesses on glass substrates are shown in Fig. 1. The XRD patterns were matched with ASTM card number C01-080-0019. The main reflections are similar, where (1 1 1) plane corresponds to the cubic system in the thin films growth. Intensities of reflections corresponding to the planes in different samples are different. However the strong reflections in all the samples indicates crystallites corresponding to the (1 1 1) plane of cubic CdS ($a = 5.82$ Å) [24]. The average crystallite size 'd' of polycrystalline materials can be estimated by applying the Scherrer formula.

$$d(\text{Å}) = \frac{k\lambda(\text{Å})}{D\cos\theta} \quad (1)$$

where the Scherrer constant k is taken equal to 0.9 [25], D is the FWHM in radians and θ is the Bragg angle in degrees corresponding to the maximum peak intensity. The calculated crystallite sizes of samples were found in the range of 140–199 nm. Generally the crystallite size depends on the substrate temperature, deposition rate, film thickness and annealing temperature [26]. XRD spectra of silver-doped CdS thin films are shown in Fig. 2. In Ag-doped CdS samples all reflections are similar to those of as-deposited CdS thin films, except one reflection around 2θ of 36.806°, corresponding to the (2 0 0) plane of cubic Ag_2S [27]. The mass% of Ag in this sample is about 5% observed by the EDX.

3.2. Surface study

SEM micrographs of as-deposited CdS thin films are given in Fig. 3. These micrographs are given with increasing order of the film thickness. Average grain sizes of the as-deposited thin films are taken from the SEM graphs and presented in Table 2. It can be clearly seen that the empty spaces are distributed throughout the micrograph, however these empty spaces were gradually reduced during the annealing process. The reduction phenomenon in the size of empty spaces may be continued if annealing time would have increased. To confirm that the observed voids were not real pores (throughout hole), the particular area of a sample was further studied by EDX.

Generally, with increasing thickness of the films the average grain size is increased with decreasing grain density [28], as shown in Table 2. It shows that with increasing thickness, thin film grows better with fewer defects and stresses resulting larger grains. The small amount of defects shows good crystallinety in grown CdS thin films. The dislocation density 'δ' has been estimated using the following equation:

$$\delta = \frac{1}{D^2} \quad (2)$$

where D is the grain size of thin film.

Silver-doped samples with different mass% ratios were characterized to study the surface morphology. SEM micrographs were taken with increasing silver content are shown in Fig. 4. The mass% ratio of the Cd, S and Ag were determined by using EDX. As far as the as-deposited CdS thin films were concerned, all grains are roughly of similar size; however after silver doping the grains became irregular and diverse in sizes.

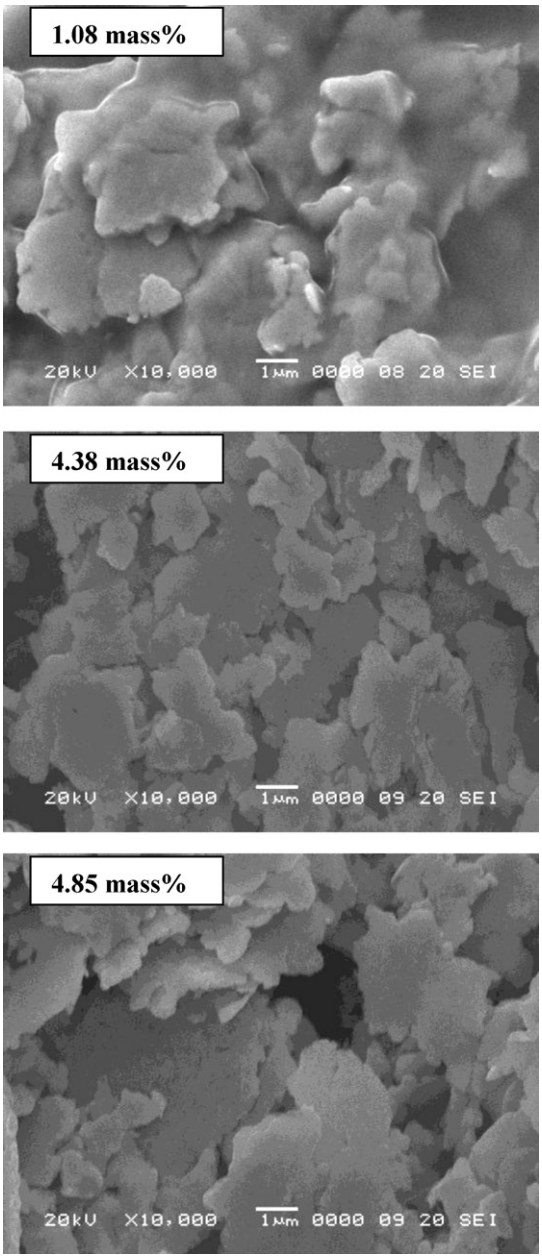

Fig. 4. SEM micrographs of silver doped CdS samples of different silver mass.

In the ion exchange mechanism, the doped species can be added into the parent material at interstitial sites and/or substitution sites depending upon the size of atoms and sites available and the phenomenon may be explained with interstitial-substitution diffusion with kick-out mechanism. As the silver ions start diffusing and set themselves at interstitial sites and later on displace some of Cd-atoms. Then Ag-ions become self-interstitial into the CdS lattice by forming Ag_2S. The process of forming Ag_2S crystallization is supported by the annealing process. From SEM micrographs of samples 1 and 2, significant increase in grain sizes was observed after Ag-doping and also the surface lost some of its smoothness. The silver-concentration also varies; it is expected that the upper layer (Ag-enriched) has a minute thickness as compared to the thickness of the whole sample. EDX graphs showing elemental ratios Cd, S and Ag are shown in Fig. 5.

Table 1
Compositional and thickness measurements of samples.

Sample name	Thin film deposition time (min)	Thickness (nm)	Ag immersion time (min)	Ag (wt%)	Composition (Cd/S)
1	5	248	1	1.08	75.74/24.25
2	6	270	5	1.99	78.18/21.82
3	7	366	10	3.02	76.45/23.55
4	8	369	15	4.38	77.00/23.00
5	10	444	20	4.65	78.87/21.13
6	15	776	25	4.86	77.51/22.49
7	18	860	30	5.09	77.04/22.96

Table 2
Variation of grain size and density with film thickness.

Sample name	Thickness (nm)	Average grain size (nm)	Dislocation density (δ) (lines/m^2)	Grain density (grains/m^2)
1	248	195.7	26.1×10^{12}	15.2×10^{12}
2	270	240.3	17.3×10^{12}	7.63×10^{12}
3	366	228.3	19.1×10^{12}	14.1×10^{12}
4	369	303.4	10.8×10^{12}	8.18×10^{12}
5	444	306.9	10.6×10^{12}	7.01×10^{12}
6	776	365.4	7.4×10^{12}	4.68×10^{12}
7	860	409.5	5.9×10^{12}	3.5×10^{12}

During sublimation process, at higher temperature CdS compound dissociates itself into Cd and S. At substrate temperature, chemical bonding again takes place and CdS compound is again formed. Due to various factors, ratio of Cd and S varies for different samples. Elemental composition of CdS thinfilms according to the EDX data is shown in Table 1. EDX analysis also confirms the assumption about the presence of voids in SEM micrographs. The EDX data for that particular region (voids) the mass% ratio was approaching the mass% obtained for the complete area scan.

3.3. Optical analysis

The study of optical properties such as transmission, refractive index and energy gap are of great importance in opto-electronics applications. The UV-VIS-NIR spectrophotometer (Perkin Elmer Lambda 950) with UV-WinLab software was used to measure the transmission spectra. The transmission spectra of as-deposited samples are shown in Fig. 6. The as-deposited CdS thin films of various thicknesses have transmission ranging from 50 to 80% in visible region. The ultraviolet region is absorbed due to having more energy than the energy band gap of cadmium sulfide, however the entire visible and near infrared region is transmitted. Therefore, cadmium sulfide is considered as a window material for the visible as well as the infrared region. Helping with Swanepoel model [29], the refractive index n can be calculated by using equation:

$$n = \frac{[N + (N^2 - 4s^2)^{1/2}]}{2} \tag{3}$$

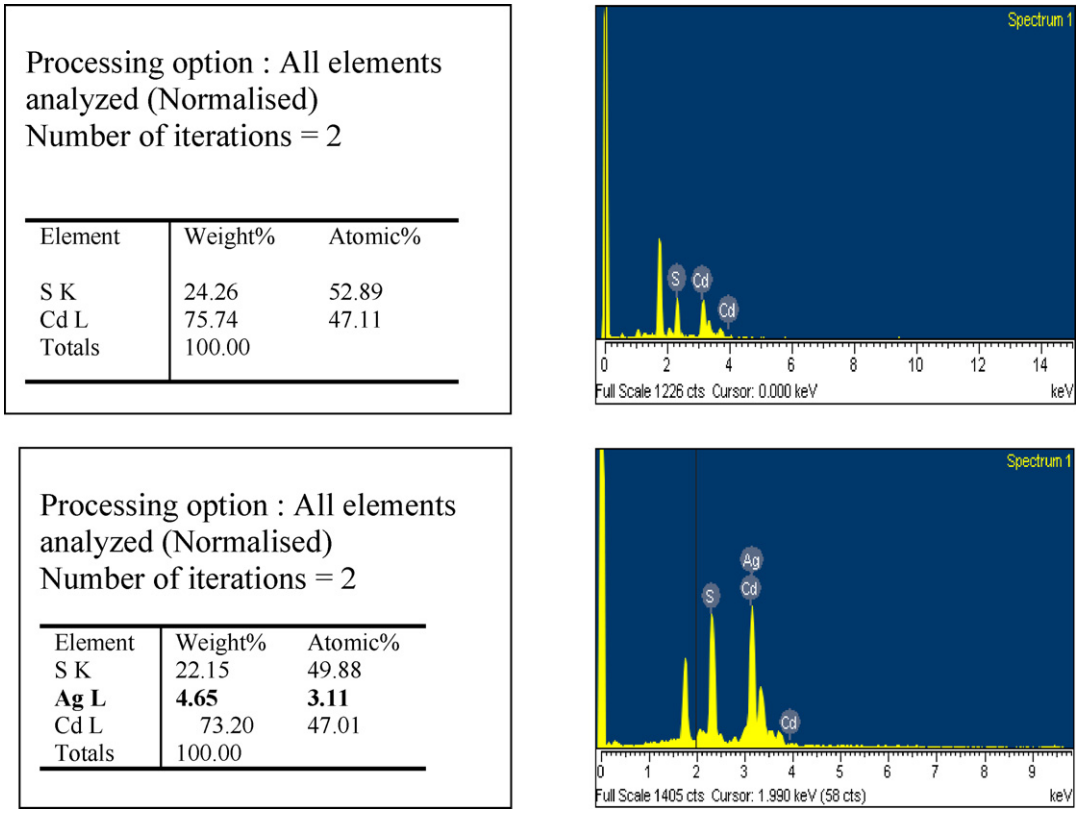

Fig. 5. EDX compositional analysis of as-doped and silver doped samples.

Table 3
Optical parameters of CdS samples.

Sample name	λ_{max} (nm)	λ_{min} (nm)	T_{max}	T_{min}	N	n
1	1620	1065.57	0.78	0.55	6.47	3.14
2	1700	1000	0.65	0.55	4.93	2.25
3	1689.69	1112.22	0.79	0.65	4.89	2.23
4	1697.16	1081.43	0.73	0.63	4.56	2.02
5	1197.11	958.29	0.66	0.52	5.69	2.69
6	1689.69	1427.54	0.75	0.55	6.16	2.97
7	1628.12	1365.97	0.77	0.61	5.29	2.47

where s is refractive index of the substrate, N is number of oscillations.

$$N = 1 + s^2 + 4s\left(\frac{T_M - T_m}{T_M T_m}\right) \quad (4)$$

where T_M and T_m are the transmission maxima and minima, respectively. Thickness of the films can be calculated by using the formula:

$$d = \frac{1}{4n}\left[\frac{\lambda_m \lambda_M}{\lambda_M - \lambda_m}\right] \quad (5)$$

where d is the thickness λ_m is the minima and λ_M is the maximum value of the wavelength taken from the transmission curves. The refractive index and thickness of thin films were calculated for all as-deposited thin films samples and given in Table 3. Refractive indices depend upon wavelength of light passing through the medium and plot of refractive index as a function of wavelength for as-deposited sample 2 thin film is shown in Fig. 7. Thickness calculated with the help of spectrophotometer was also verified by SEM image as shown in Fig. 8.

The energy band gap was calculated by finding out the particular point, where transmission abruptly increases. The band gap can be calculated by using the equation:

$$E_g = \frac{hc}{\lambda} \quad (6)$$

It is observed that with increase in film thickness, values of band gap slightly decreased. The transmission of thin films has been decreased from 80 to 40% after silver doping as shown in Fig. 9. With increasing silver mass%, the samples' transmission is gradually decreased causing increase in refractive index. There is no significant change observed in band gap after doping of silver [30], however the band gap may be changed with larger amount of silver doping.

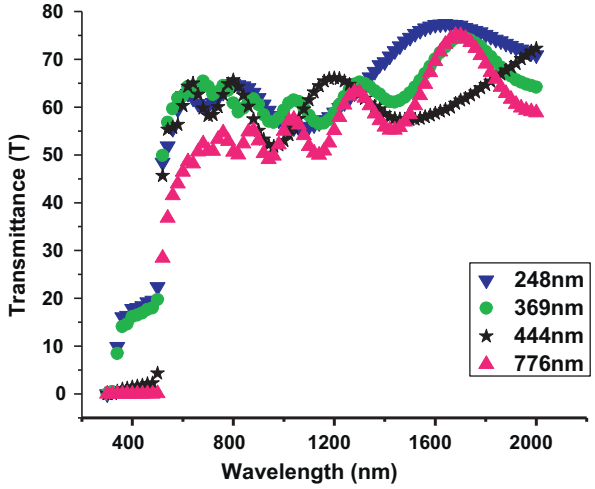

Fig. 6. Transmission curves of as-deposited CdS samples with variation in thickness.

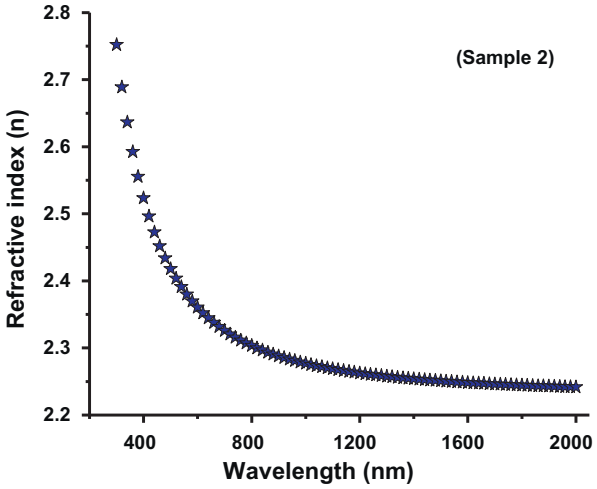

Fig. 7. Plot of refractive index versus wavelength of a CdS sample.

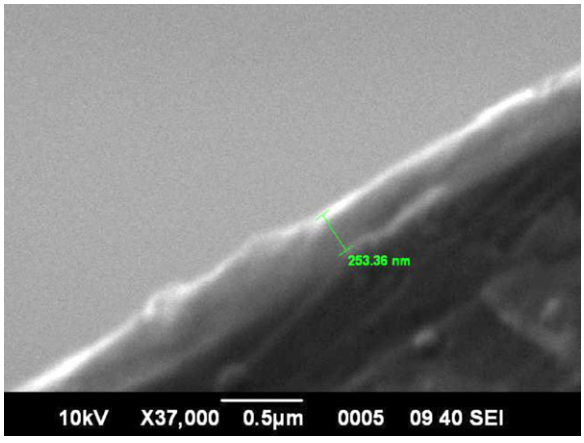

Fig. 8. SEM image side-view of CdS sample.

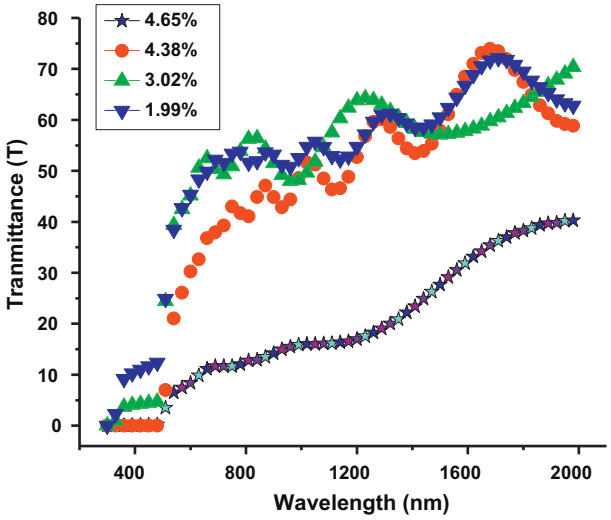

Fig. 9. Plot of transmission curves of silver-doped CdS samples.

4. Conclusions

Thin films of CdS prepared by thermal evaporation technique showed polycrystalline structure with preferred growth in ⟨1 1 1⟩ direction. Structural investigations showed that average grain size increased from 195.7 nm to 409.5 nm with increase in film thickness from 248 nm to 860 nm, respectively. Different microstructures show that the post annealing and silver doping strongly affects the morphology of the samples. When the films were immersed into low concentrated silver nitrate solution, samples remained in the solution for longer time without being damaged. Diffusion of silver into the films occurred by annealing. Optical study showed that optical transmission decreased with increase in silver mass% because silver is a good reflector. Transmission decreased from 80% to 30% as samples were doped with silver. A slight shift in optical band gap was observed. The refractive indices range from 2.02 to 3.14 and corresponding thickness varies from 248 nm to 860 nm.

Acknowledgements

The authors would like to thank HEC, Pakistan for financial support through project 20-1187/R&D/09 and COMSATS Institute of Information Technology, Islamabad. The authors would also like to thank Manzar Abbas of CIIT, Islamabad for continuous support and valuable discussion.

References

[1] R. Tenne, V.M. Nabutovsky, E. Lifshitz, A.F. Francis, Solid State Commun. 82 (1992) 651.
[2] V. Ruxandra, S. Antohe, J. Appl. Phys. 84 (1998) 727.
[3] B. Su, K.L. Choy, Thin Solid Films 102 (2000) 361.
[4] A.G. Valyomana, K.P. Vijayakumar, C. Purushothaman, J. Mater. Sci. Lett. 11 (1992) 616.
[5] H. Chavez, M. Jordan, J.C. McClure, G. Lush, V.P. Singh, J. Mater. Sci. 8 (1997) 151.
[6] F. Izci, S. Kose, K. Yckaya, Proc. Suppl. Bpl. 5 (1997) 1115.
[7] A.G. Valyomana, K.P. Vijayakumar, C. Purushothaman, J. Mater. Sci. Lett. 9 (1990) 1025.
[8] S.A. Al Kuhaimi, Vacuum 51 (1998) 349.
[9] I. Gunal, M. Parlak, J. Mater. Sci. 8 (1997) 9.
[10] U.U. Pal, R. Silva-Gonzalez, G. Martinez-Montes, M. Gracia Jimenez, M.A. Vidal, S. Torres, Thin Solid Films 305 (1997) 345.
[11] H. Zhang, X. Ma, D. Yang, Mater. Lett. 58 (2003) 5.
[12] J. Pantoja, X. Mathew, Sol. Energy Mater. Sol. Cells 76 (2003) 313.
[13] M.E. Ozsan, D.R. Johnson, M. Sadeghi, D. Svapathasundaram, G. Goodlet, M.J. Furlong, L.M. Peter, A.A. Shingleton, J. Mater. Sci. 7 (1996) 119.
[14] N. Romeo, A. Bosio, R. Dedeschi, V. Canevari, Thin Solid Films 327 (2000) 361.
[15] R.N. Ahmad-Bitar, Renew. Energy 19 (2000) 579.
[16] H. Ariza-Calderon, R. Lozada-Morales, O. Zelaya-Angel, J.G. Mendoza, L. Banos, J. Vac. Sci. Technol. 14 (1996) 2480.
[17] S.J. Ikhmayies, Production and Characterization of CdS/CdTe Thin Film Photovoltaic Solar Cells of Potential Industrial Use, Ph.D. Thesis, University of Jordan, 2002.
[18] O. Vigil, I. Riech, M. Garcia-Rocha, O. Zelaya-Angel, J. Vac. Sci. Technol. 15 (1997) 2282.
[19] O. Melo De, L. Hernan ĭ dez, O. Zelaya-Angel, R. Lozada-Morales, M. Bercerril, E. Vasco, Appl. Phys. Lett. 65 (1994) 1278.
[20] M. Lepek, B. Dogil, Thin Solid Films 109 (1983) 103.
[21] B. Ullrich, R. Schroeder, IEEE J. Quantum Electron. 37 (2001) 1363.
[22] H. Wang, Y. Zhu, P.P. Ong, J. Cryst. Growth 220 (2000) 554.
[23] M. Khanlary, P. Townsenda, B. Ullrich, D.E. Hole, J. Appl. Phys. 97 (2005) 23512.
[24] J. Magn. Magn. Mater. 152 (1996) 159.
[25] V. Kapaklis, P. Poulopoulos, V. Karoutsos, T. Manouras, C. Politis, Thin Solid Films 510 (2006) 138.
[26] K.L. Chopra, Thin Film Phenomena, McGraw-Hill, New York, 1969.
[27] Z. Leipzig, Phys. Chem. 31 (1935) 157.
[28] J.P. Enrquez, X. Mathew, Sol. Energy Mater. Sol. Cells 76 (2003) 313.
[29] R. Swanepoel, J. Phys. E: Sci. Instrum. 6 (1983) 1214.
[30] N.A. Shah, A.K.S. Aqili, A. Maqsood, J. Cryst. Growth 290 (2006) 452.